

**FATIGUE LIFE PREDICTING FOR NITRIDED STEEL – FINITE ELEMENT ANALYSIS**

Thermo-chemical treatments are known to increase the fatigue life of industrial parts. Due to the imprecise consideration of residual stresses in predicting the durability of components subjected to cyclic loading and their effect on the fatigue life, the authors developed a numerical model combining the influence of residual stresses with stresses caused by bending. The authors performed the numerical simulation with the use of Finite Element Method to analyse material behaviour during cyclic loading. The residual stress state developed during nitriding was introduced onto cross-section of the numerical specimen. The goal of this work was better understanding of the real conditions of the nitride steel fatigue processes and improving the knowledge about numerical predicting of the fatigue life for parts with residual stresses. The results of simulation were compared with plane bending fatigue tests. The presented method indicates the possibility of increasing the accuracy of the fatigue analysis of elements after surface treatment, increasing its certainty and the ability to perform better optimization of service life.

*Keywords:* numerical simulation, nitriding, fatigue life, fatigue analysis, finite element

**1. Introduction**

Nitriding is one of the most widely used kinds of thermo-chemical treatment. Numerous studies have shown that the nitriding process has a significant impact on the expected fatigue life of elements. The state of residual stresses in the nitrided layer results in the initiation of cracks under the surface rather than on the surface, which was described by way of example with maraging steel by Hussain and others [1]. Farkohzadeh and Edrissy demonstrated the improvement of fatigue properties of nitrided titanium alloy elements [2]. Experimental results for nitrided austenitic steel elements obtained by Celik and others showed an increase in the fatigue limit by 15% in relation to unnitrided samples [3]. Guagliano and Vergani showed in their studies that along with time elongation of the nitriding process, the low-cycle material strength decreases due to the occurrence of a white layer [4]. In their studies, Hassani-Gangaraj and others showed that plasma nitriding significantly improves the low-alloy steel fatigue limit [5]. The similar experimental results were obtained by Winck and others for stainless steel [6], and by Terres and others for 42CrMo4 steel [7].

The traditional approach to fatigue analysis requires the possession of fatigue properties characterising the selected material behaviour according to the load repetition amplitude level. The correct assessment results of fatigue properties are obtained from the regression of results of a series of fatigue tests performed on smooth (perfect) type samples [8]. Then, the information is modified by the strength correction factors,

depending on the average cycle stress value, environment aggressiveness, surface roughness, stress state gradient, as well as heat and thermo-chemical treatments. The last factor is very important, because compressive residual stresses cause an additional specific shift of the average cycle stress, which results in a significant increase in durability. In the literature [9,10], it is possible to find overall values of correction factors of the fatigue limit change. However, these factors refer to the very fact of the thermo-chemical treatment existence, except for exact values of the state of residual stresses.

The current calculation technology provides possibilities that were previously unreachable with analytical methods. The use of numerical methods, especially the Finite Element Method (FEM), allows to more accurately predict the strength of machines, and therefore, to improve the quality of manufactured products. The FEM method has already been used in the works of Gawroński and Sawicki [11,12] in order to predict the impact of thermo-chemical treatment on the durability of elements and machine parts. Xin and others used a three-dimensional model of FEM in a fatigue simulation of railway switches [13]. Nourbakhshnia and Liu used an innovative method in order to simulate the development of fatigue cracks (a singular edge-based smoothed finite element method – ES-FEM) [14]. The method of finite elements was also used to predict the strength of composite materials in the studies of Paepegem and others [15] as well as Wu and others [16]. Morishita and Itoh used FEM for steel sample testing under the cyclic disproportionate load [17].

\* LODZ UNIVERSITY OF TECHNOLOGY, INSTITUTE OF MATERIALS SCIENCE AND ENGINEERING, STEFANOWSKIEGO 1/15, 90-924 LODZ, POLAND

# Corresponding author: jacek.sawicki@p.lodz.pl

Due to the vague consideration of the residual stresses in predicting the durability of elements subject to cyclic loads and their impact on the fatigue life, the authors developed a numerical model combining residual stresses generated with the use of the methodology described in one of Sawicki's previous works [18,19] with stresses caused by bending. The authors established the following hypothesis of the fatigue strength prognosis. The element fatigue strength after thermo-chemical treatment, e.g. nitriding, can be determined by using fatigue properties of the material before treatment, corrected by the state of remaining stresses, i.e. residual stresses with reference to their plastic redistribution and stress state gradient.

Mesh and its quality has a very strong influence on the performance of the numerical model. The process of mesh optimisation includes finding the best element sizing, refining mesh at certain places and comparing the results. Mesh sensitivity studies should be always performed when working on the new numerical, finite element model. An example of such a study was shown in an article by Guo et al. describing their three-dimensional fracture model [20]. Another example can be found in the work by Castelluccio and McDowell [21] showing mesh refinement influence on Fatigue Indicator Parameters. Madej and Szyndler performed analysis of the influence of mesh density on the quality of obtained results in plane strain deformation [22]. Some authors use adaptive mesh generation to obtain best results, like Kruzel et al. in their multiscale applications [23].

## 2. Research methodology

Fatigue tests for 42CrMo4 tempered steel were preceded by static tests. The aim of this research was to identify static properties of the samples' materials (Fig. 1) and initially determine the variable load levels. During static tests, a special instrument for testing the strength under the flat-bending conditions was used (Fig. 2). The manufactured instrument was mounted in the grips of a universal testing machine. The instrument provided a constant bending moment on the loaded sample measuring part. The sample deformations were measured with the use of an extensometer on the measuring basis of 25 mm, which is included in the universal testing machine. The extensometer was mounted on the measuring part of samples (Fig. 2). The sample was loaded at a rate of the piston shift of 0.1 mm/s. During the tests, instantaneous loading force values and sample deformations were recorded.

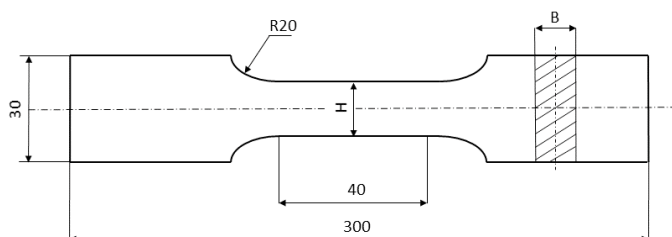


Fig. 1. Samples used for testing

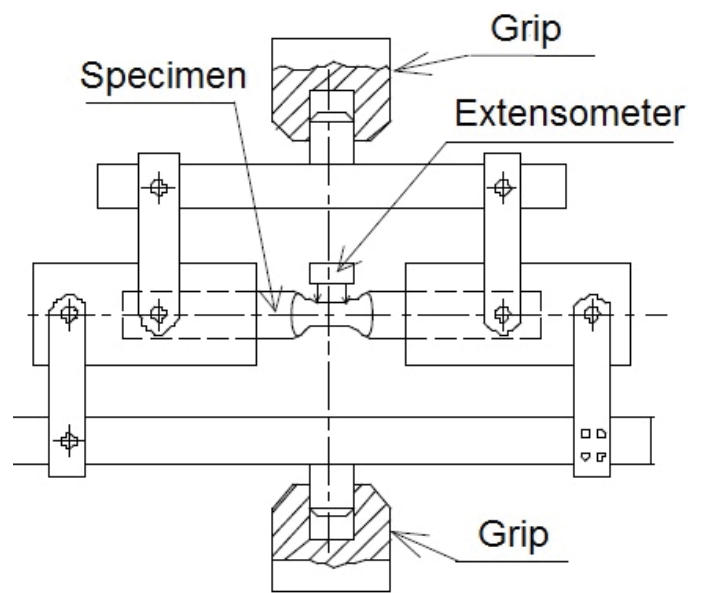


Fig. 2. Diagram of a device for static and fatigue tests under flat-bending conditions

Fatigue tests were carried out on flat samples intended for flat-bending testing according to the standard [8] (Fig. 1). The samples were mounted in the grip for two-point bending (Fig. 2), and then, they were subject to variable swinging loads. The grip provides a constant bending moment on the measuring cross-section. Six samples were tested in terms of a stress amplitude range  $\sigma_{ai}$  from 400 MPa to 1000 MPa, with a leap every 100 MPa. During testing, the load frequency was 4 Hz. The tests were performed at 21°C. The target zone extension was measured by the extensometer while recording the force on the universal testing machine piston. A 10% increase of the universal testing machine piston displacement in relation to the piston displacement for the fatigue test constant conditions was assumed as a criterion of the test end. During fatigue tests, instantaneous values of the force loading the sample as well as its deformation for the selected variable load cycles were recorded.

## 3. Static and fatigue test experimental results

The loading force instantaneous values and sample deformations recorded during static testing allowed us to perform a graph of bending in the coordinate system of bending stresses – sample measuring part deformation. Instantaneous bending stresses  $\sigma_g$  were calculated by dividing the value of the  $M_g$  instantaneous bending moment by the  $W_x$  ratio of cross-section sample of the measuring part. The obtained bending graph was shown in Fig. 3. Fig. 4 shows damage forms of the tested samples during the static bending test.

Despite the cracks that occurred on the surface (Fig. 4b), the 42CrMo4 steel sample was not subject to permanent separation. The depth of the occurred cracks was up to a few millimetres. On the basis of an analysis of the 42CrMo4 steel sample fracture, it can be concluded that during the static test, the sample

surface layer cracked. The plastic core allowed for substantial deformations during the static test without separation of the measuring section.

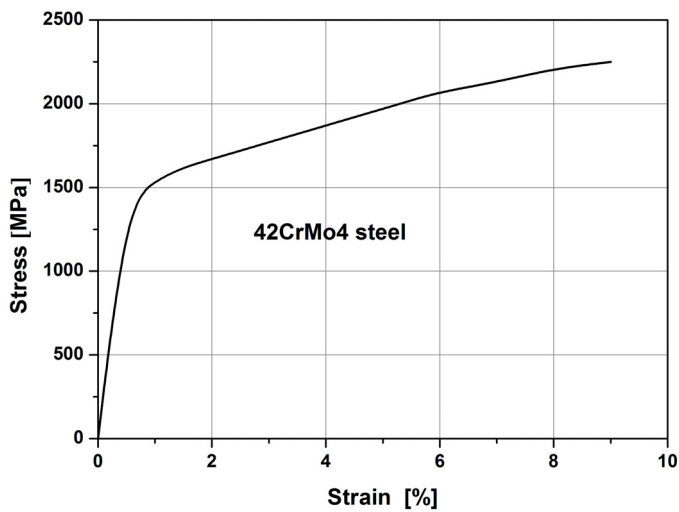


Fig. 3. Graphs of 42CrMo4 tempered steel static bending

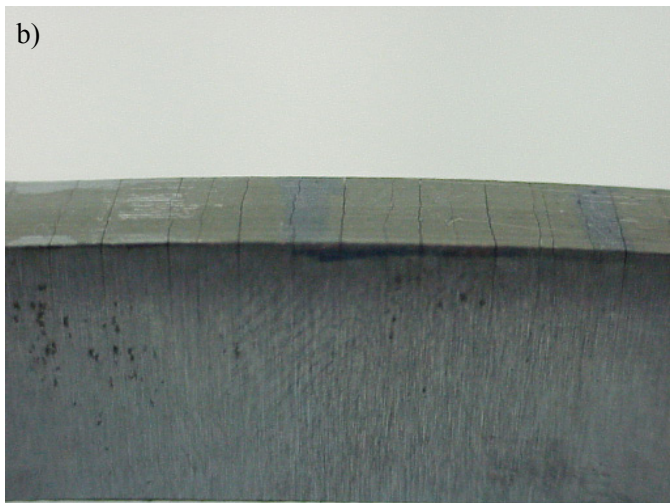
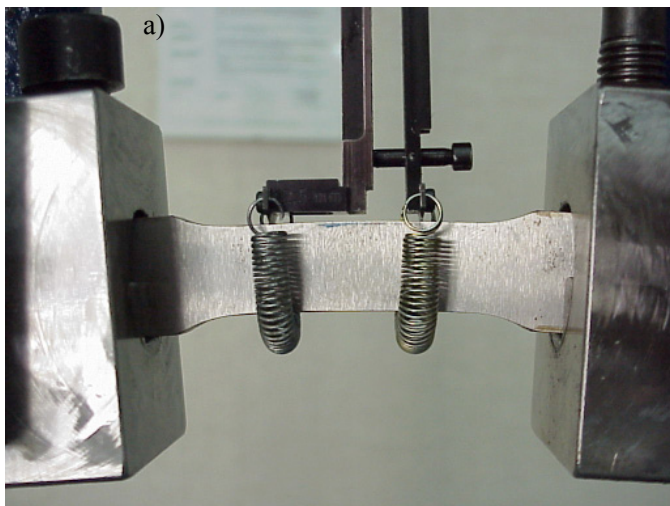


Fig. 4. The damage form of 42CrMo4 steel samples at the end of a static bending test: a) sample views, b) form of cracks on the sample surface

Based on the fatigue tests of the 42CrMo4 steel samples, it was found that regardless of the stress level, the sample is subject to cyclic creep. The phenomenon involved a hysteresis loop movement along the axis of abscissae. While analysing the results, attention was paid to two quantities, i.e. a range of the  $\Delta\varepsilon$  sample deformation changes as well as the  $\varepsilon_{\max}$ , maximum deformation and the  $\varepsilon_{\min}$  minimum deformation measured with the use of the extensometer. During the cyclic creep, the coordinates of the loop's recorded characteristic points change, i.e.  $\varepsilon_{\max}$ ,  $\varepsilon_{\min}$ . The loop movement range on the axis of abscissae is affected by the stress level. Higher deformation values  $\varepsilon_{\max}$ ,  $\varepsilon_{\min}$  are obtained at higher levels of stress. In order to assess the course of deformation changes during loading, Figure 5 shows the course of maximum and minimum deformations in a function of the number of load cycles at two stress levels:  $\sigma_a = 800$  MPa,  $\sigma_a = 500$  MPa.

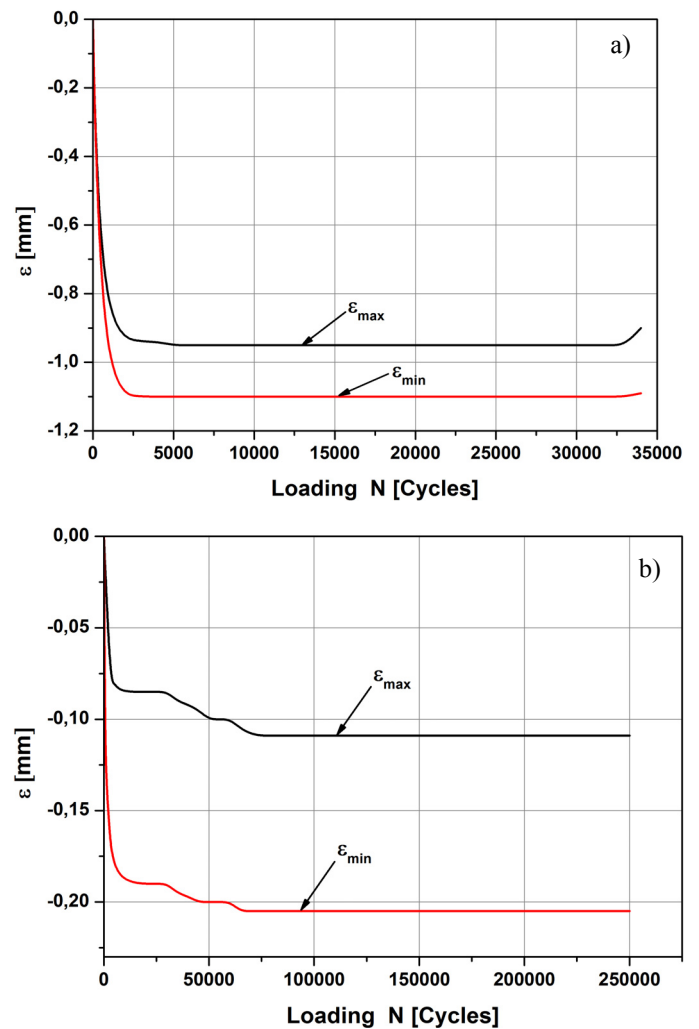


Fig. 5. Changes in the  $\varepsilon_{\max}$  maximum and  $\varepsilon_{\min}$  minimum deformations at two levels of the constant amplitude load of 42CrMo4 steel samples: a)  $\sigma_a = 500$  MPa, b)  $\sigma_a = 800$  MPa

On the basis of the analysis of graphs presented in Fig. 5, it can be concluded that the intensity of the course of cyclic creep depends on the degree of fatigue damage. The highest intensity applies to the first durability period and covers about 20% of

the total number of cycles to the fatigue crack. It relates both to the lowest performed stress levels and also to the highest levels.

During fatigue tests of the 42CrMo4 steel samples, the occurrence of changes in cyclic properties was not found. The confirmation of this fact seems to include slight changes in the range of the  $\Delta\varepsilon$  deformation changes. The analysis of the implemented graphs allows us to conclude that, except for short periods at the beginning and at the end of testing, there is a stabilisation of the deformation range. It applies to all the analysed load levels.

The numbers of cycles for cracking of samples obtained at individual  $\sigma_a$  stress levels were approximated in the system of logarithmic coordinates by a straight line of the fatigue graph defined by the equation of the following form:

$$\log \sigma_a = \sigma_a \log N + b$$

where:  $a$  – slope of straight regression,  $b$  – absolute term of straight regression.

The obtained results listed in the form of a fatigue graph were shown in Figure 6. The  $Z_{go}$  fatigue limit for the 42CrMo4 steel samples was determined in accordance with the equation of the fatigue graph for a base number of  $N_g = 5 \times 10^6$  cycles. A list of mechanical properties was presented in Table 1.

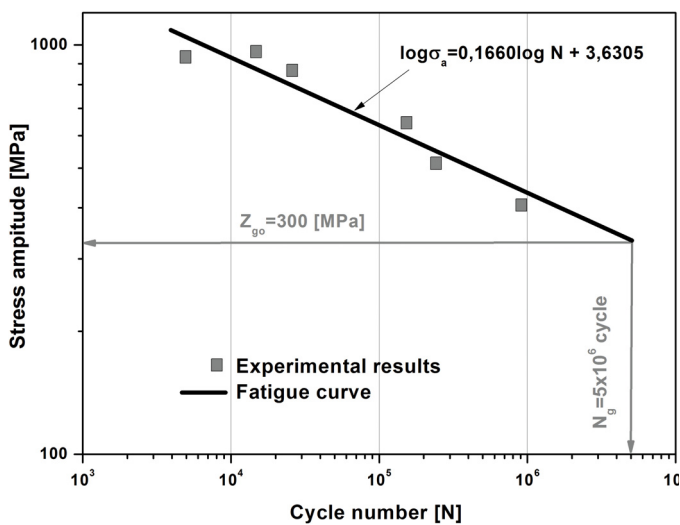


Fig. 6. Fatigue graph for 42CrMo4 steel samples

TABLE 1

42CrMo4 steel mechanical properties

$R_e$ [MPa]	$R_m$ [MPa]	$E$ [MPa]	$Z_o$ [MPa]	$b$
1030	880	2e5	330 (N = 5e6 cycles)	3,63

#### 4. Numerical prediction of durability

The durability prognosis presented below assumes a hypothesis that the element fatigue strength after nitriding treatment can be determined by using fatigue properties of the material before treatment, corrected by the state of remaining stresses, i.e. residual stresses with reference to their plastic redistribution and stress state gradient.

#### 4.1. Numerical model

In the first stage, a two-dimensional discrete model was created (Fig. 7). Due to the shape of the sample, the thickness dimension of which is much smaller than the others, it was decided to adopt the description using a plane stress state (PSS). The surface geometry was adopted by cutting the sample lengthwise. In the mathematical model, a mesh of finite elements aimed at the correct capture of the gradient of stresses in the surface layer was applied. In this case, the depth of the layer hardened by nitrogen was 0.1 mm. It was assumed that elements under the surface of the sample increase every 30 layers by a multiplication of 1.1 from the size of 5  $\mu\text{m}$ . Therefore, a 0.822 mm layer of enough small elements was obtained at the surface in order to accurately reflect the distribution of residual stresses in the further stages. The remaining volume was modelled by finite elements of larger sizes.

Mesh applied to the model was obtained with the developed macro introduced into ANSYS software. Said macro was created in order to check the maximum values of stresses and where they appear and also to select optimized mesh parameters to shorten the simulation time. Additionally, the numerical analysis using the submodeling option was performed to check the change in stress values in places of high stress concentration (at round edges).

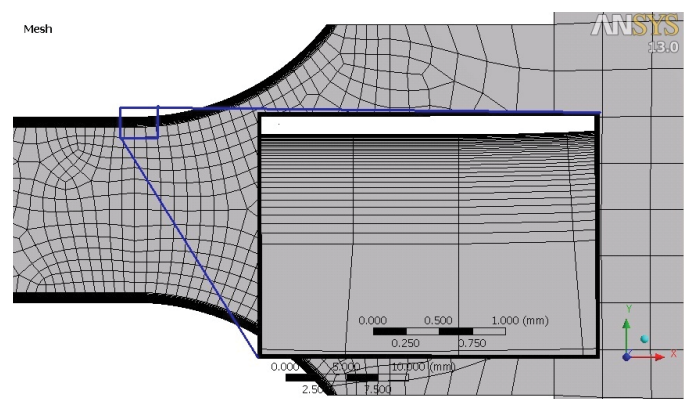


Fig. 7. Discrete model of a fatigue sample [18]

In order to implement the residual stresses, a technique presented and described in detail in the authors' other work was applied [18,19]. Then, with the use of a created macro, in the previously implemented mesh, the material variable properties were assigned to all significant flat and curvilinear surfaces. After the numerical analysis was carried out, the obtained distribution of directional stress along the  $\sigma_x$  sample (Fig. 8) was consistent with the values of stresses obtained with the Waisman-Phillips method (Fig. 9) [24].

In the next stage of simulation, based on the stress distribution results obtained from the FEM model, the fatigue analyses were carried out. In the analysis, any correction factors of the fatigue limit were applied assuming that the sample before and after the process remains perfectly smooth. In order to compare

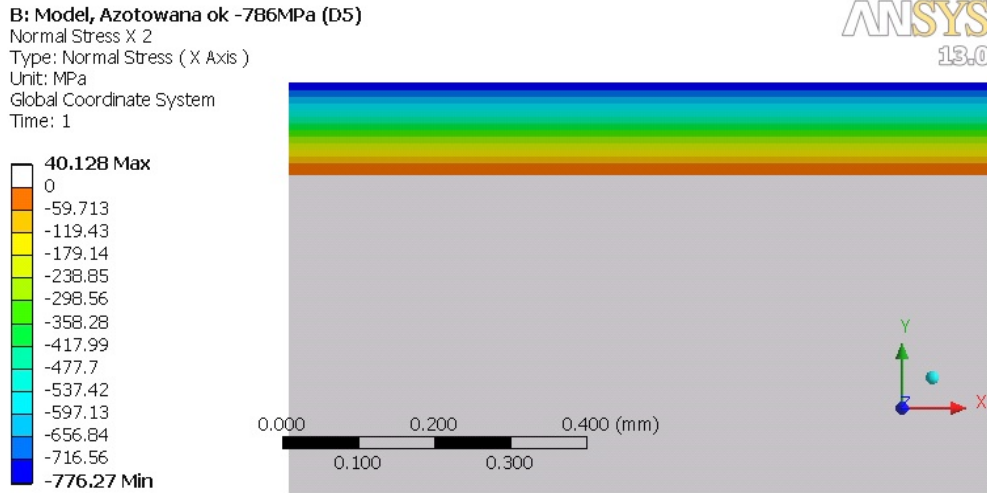


Fig. 8. Map of distribution of residual stresses in a nitrided sample [18]

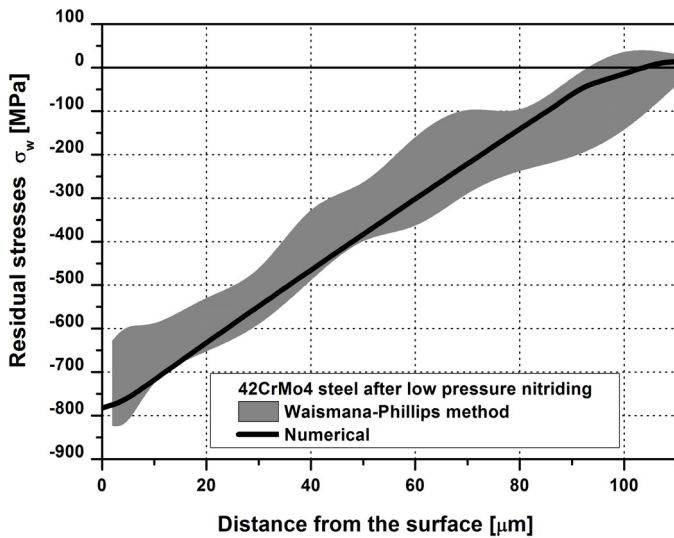


Fig. 9. Distribution of residual stresses in 42CrMo4 steel after low pressure nitriding

the cases of the tempered and nitrided materials, an endurance test curve presenting the base material characteristics was used. The data was entered into the programme, in which a durability calculation was made.

A numerical analysis of the stress state at cyclic loading was conducted on three load levels with the bending force, acting in the Y axis on the arm of 177 mm with the following values: 5250 N, 4725 N and 4200 N. Fig. 10 shows the distribution of stresses resulting from a bending moment of 929 Nm.

As a result of the carried out fatigue calculations, the distribution maps of the amplitude of breaking stresses and the fatigue life were obtained (Figs. 11-14). It can be noticed that the maximum value for a nitrided element is 529 MPa, and in the case of a tempered element, it is 510 MPa. The biggest difference between these two samples occurs on the nitrided sample surface. It is reflected in the fatigue life listed in Figs. 13 and 14.

The comparison of durability on the cross-section in the form of graphs in Fig. 15 illustrates the local improvement of

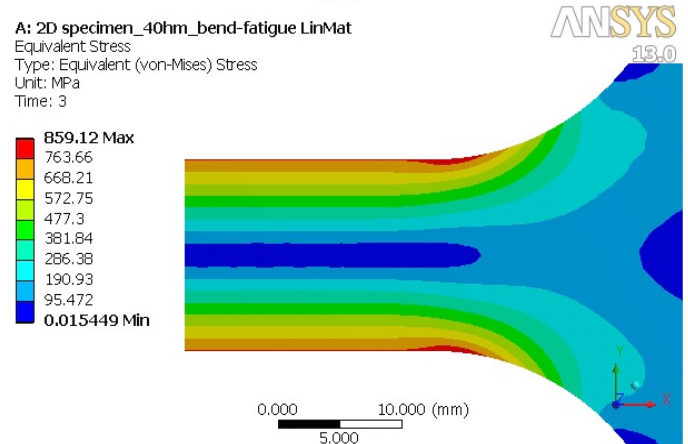
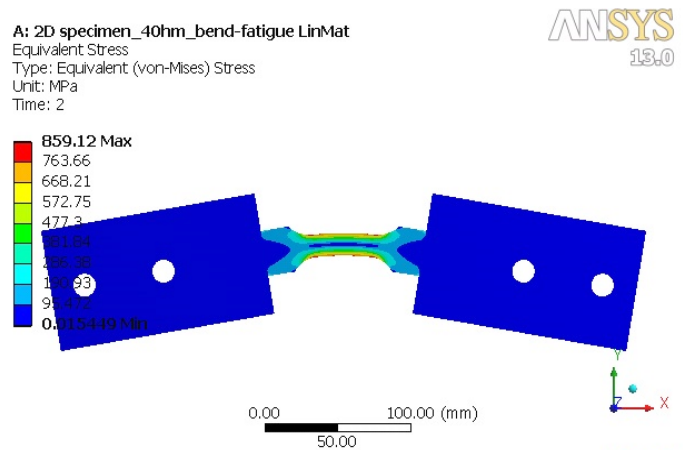


Fig. 10. Stress state on a tempered sample cross-section after a bending moment loading [18]

durability on the surface of samples after the nitriding process. The increase in durability results from the existence of a component of the constant compressive stress. This component moves the fatigue curve for the nitrided material by a constant value of the stress amplitude, which is the effect of the obtained state of residual stresses.

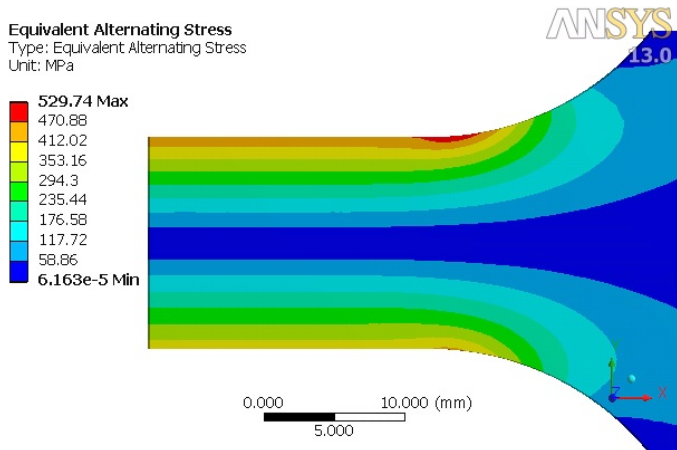


Fig. 11. Map of the stress amplitude in a tempered element under  $F = 5250$  N one-sided loading [18]

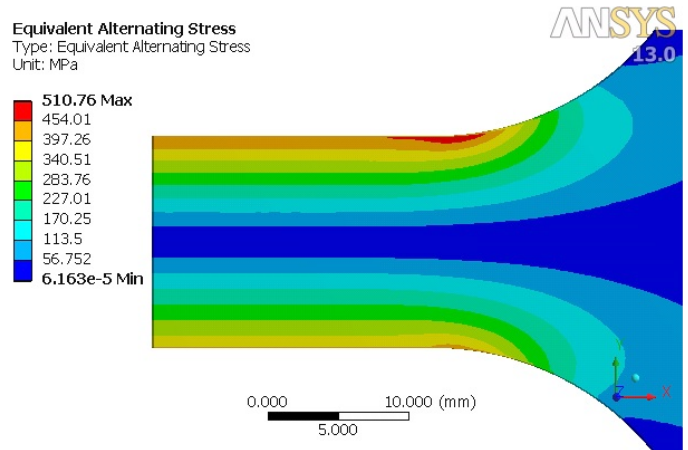


Fig. 12. Map of the stress amplitude in a nitrided element under  $F = 5250$  N one-sided loading [18]

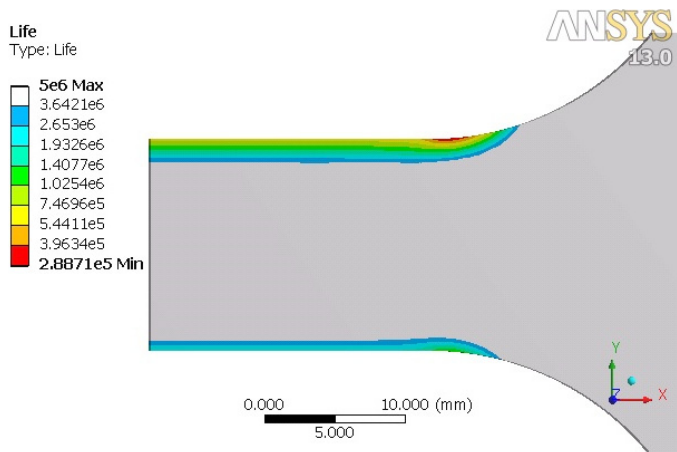


Fig. 13. Fatigue life of a tempered element under  $F = 5250$  N one-sided loading [18]

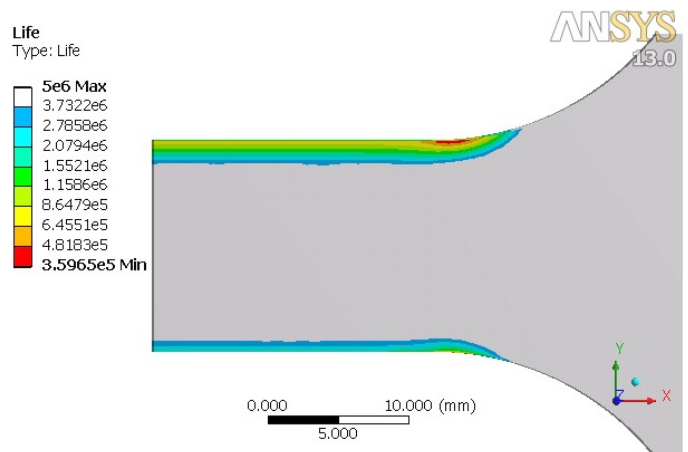


Fig. 14. Fatigue life of a nitrided element under  $F = 5250$  N one-sided loading [18]

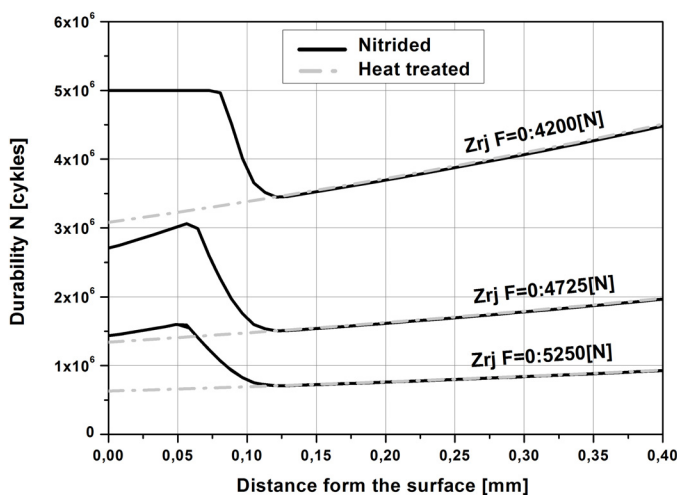


Fig. 15. Fatigue life change of nitrided elements in relation to tempered elements for one-sided bending [18]

### 5. Conclusions

The presented method shows the possibility of increasing the fatigue analysis accuracy of elements after surface treatment, increasing confidence of their implementation and the possibility of their better optimisation in terms of service life.

The simulation of distribution of residual stresses is essential for predicting the durability of tempered elements or conscious shaping of surface layers in order to ensure durability in specific operating conditions.

The proposed methodology allows for the synergistic combination of an effect of the surface layer obtained properties (residual stresses) with the simulation of “extortion”, to which it will be subjected in actual operating conditions. It may include guidelines for technologists on how to modify the process of generating a new surface layer, in order to achieve a similarly beneficial effect in reality.

The adopted numerical model of estimating the distribution of residual stresses in nitrided layers was experimentally verified with a fairly good correlation. Undoubtedly, the convergence of numerical simulation with the given experiments will be

increasingly larger on subsequent repetitions, but the improvement of this compatibility should be found in clarification and verification of the assumptions adopted as a basis for modelling.

The carried-out analysis constitutes its first stage and a good basis to continue the works on the characterisation of a three-dimensional state of residual stresses that occurs at the sample cross-section and the use of a model of the elastic-plastic material with reinforcement.

#### REFERENCES

- [1] K. Hussain, A. Tauqir, A. ul Haq, A.Q. Khan, *Int. J. Fatigue* **21** (2), 163-168 (1999).
- [2] K. Farokhzadeh, A. Edrisy, *Mater. Sci. Eng. A* **620**, 435-444 (2015).
- [3] O. Celik, M. Baydogan, E. Atar, E.S. Kayali, H. Cimenoglu, *Mater. Sci. Eng. A* **565**, 38-43 (2013).
- [4] M. Guagliano, L. Vergani, *Int. J. Fatigue*, **19** (1), 67-73 (1997).
- [5] S.M. Hassani-Gangaraj, A. Moridi, M. Guagliano, A. Ghidini, M. Boniardi, *Int. J. Fatigue* **62**, 67-76 (2014).
- [6] L.B. Winck, J.L.A. Ferreira, J.A. Araujo, M.D. Manfrinato, C.R.M. da Silva, *Surf. Coat. Tech.* **232**, 844-850 (2013).
- [7] M.A. Terres, S. Ben Mohamed, H. Sidhom, *Int. J. Fatigue* **32** (11), 1795-1804 (2010).
- [8] ASME E 466-96 (2002) Standard Practice for Conducting Force Controlled Constant Amplitude Aerial Fatigue Test of Metallic Materials.
- [9] J.A. Bannantine, *Fundamentals of Metal Fatigue Analysis*. Publisher: Prentice Hall 1997.
- [10] J. Schijve, *Fatigue of Structures and Materials*. Publisher: Springer Netherlands 2009.
- [11] Z. Gawroński, J. Sawicki, *Mater. Sci. Forum* **513**, 69-74 (2006).
- [12] J. Sawicki, M. Górecki, L. Kaczmarek, Z. Gawroński, K. Dybowski, R. Pietrasik, W. Pawlak, *Chiang. Mai. J. S.* **40** (5), 886-897 (2013).
- [13] L. Xin, V.L. Markine, I.Y. Shevtsov, *Wear* **366-367**, 167-179 (2016).
- [14] N. Nourbakhshnia, G.R. Liu, *Inter. J. Fatigue* **40**, 105-111 (2012).
- [15] W. Van Paepegem, J. Degrieck, P. De Baets, *Compos. Part B-Eng.* **32**, 7, 575-588 (2001).
- [16] L. Wu, F. Zhang, B. Sun, B. Gu, *Int. J. Mech. Sci.* **84**, 41-53 (2014).
- [17] T. Morishita, T. Itoh, *Theor. Appl. Fract. Mec.* **84**, 98-105 (2016).
- [18] J. Sawicki, Modeling of multiphase systems in materials engineering, *Scientific Bulletin of the Lodz University of Technology*, No. 1129, 2012.
- [19] J. Sawicki, P. Siedlaczek, A. Staszczuk, *Met. Sci. Heat. Treat.* **59** (11-12), 799-804 (2018).
- [20] L. Guo, J. Xiang, J. Latham, B. Izzuddin, *Eng. Fract. Mech.* **151**, 70-91 (2016).
- [21] G. Castelluccio, D. McDowell, *Mater. Sci. Eng. A* **639**, 626-639 (2015).
- [22] Ł. Madej, J. Szyndler, *Comput. Mater. Sci.* **96**, 200-213 (2015).
- [23] F. Kruzal, L. Madej, K. Perzynski, K. Banas, *Int. J. Multiscale Com.* **12** (3), 257-269 (2014).
- [24] J.W. Waisman, A. Phillips, *P. Soc.* **XI/2**, 102-105 (1952).